

Simulation of PZT monitoring of reinforced concrete beams retrofitted with CFRP

C.P. Providakis^{*1}, T.C. Triantafillou², D. Karabalis², A. Papanicolaou²,
K. Stefanaki¹, A. Tsantilis² and E. Tzoura²

¹Department of Architectural Engineering, Technical University of Crete, GR-73100 Chania, Greece

²Department of Civil Engineering, University of Patras, GR-26500 Patras, Greece

(Received June 17, 2013, Revised October 20, 2013, Accepted November 9, 2013)

Abstract. A numerical study has been carried out to simulate an innovative monitoring procedure to detect and localize damage in reinforced concrete beams retrofitted with carbon fiber reinforced polymer (CFRP) unidirectional laminates. The main novelty of the present simulation is its ability to conduct the electro-mechanical admittance monitoring technique by considerably compressing the amount of data required for damage detection and localization. A FEM simulation of electromechanical admittance-based sensing technique was employed by applying lead zirconate titanate (PZT) transducers to acquire impedance spectrum signatures. Response surface methodology (RSM) is finally adopted as a tool for solving inverse problems to estimate the location and size of damaged areas from the relationship between damage and electro-mechanical admittance changes computed at PZT transducer surfaces. This statistical metamodel technique allows polynomial models to be produced without requiring complicated modeling or numerous data sets after the generation of damage, leading to considerably lower cost of creating diagnostic database. Finally, a numerical example is carried out regarding a steel-reinforced concrete (RC) beam model monotonically loaded up to its failure which is also retrofitted by a CFRP laminate to verify the validity of the present metamodeling monitoring technique. The load-carrying capacity of concrete is predicted in the present paper by utilizing an Ottosen-type failure surface in order to better take into account the passive confinement behavior of retrofitted concrete material under the application of FRP laminate.

Keywords: damage identification; structural health monitoring; electromechanical admittance; FEM; response surface metamodels; Ottosen-type concrete failure

1. Introduction

As aging of concrete material, continuous use, overloading, aggressive exposure conditions and lack of sufficient maintenance accelerate the deterioration of concrete infrastructures, fiber reinforced polymer (FRP) laminates have become an attractive alternative for concrete retrofit and rehabilitation. The attraction of using FRPs in the concrete construction industry is mainly coming from their exceptional mechanical properties such as high tensile strength, low weight, corrosion resistance, high fatigue life, flexibility in design requirements and easy of fabrication. Although the growth in their usage has been going on more and more than a quarter of century, an

*Corresponding author, Professor, E-mail: cprov@mred.tuc.gr

understanding of their long term performance still remains elusive. As a result, damage identification is of considerable importance in view of the loss of life and property that may result from structural failure. Adopting periodic inspection routines using nondestructive techniques for damage detection will essentially raise the confidence of both engineers and contractors in exploiting the full potential of FRPs' mechanical properties. Furthermore, if damage is detected and identified at early stage, then the structure may be economically repaired. Therefore, the need for quick damage detection and identification has necessitated research for the development of many structural health monitoring techniques.

The critical issue in concrete structures externally retrofitted with FRP is bond, or rather the mechanism of debonding, which represents the most commonly observed mode of failure (Oehlers 2004). One can conclude that typical examples of defects at the interface between FRP and concrete substrate are voids and delaminations. Both defects may affect the structural integrity, performance and life expectancy while in the same time, are very important for the flexural strength development of the retrofitted system (Shih *et al.* 2003 and Boukhezar *et al.* 2013). To ensure the proper functioning of concrete structures retrofitted with FRP, efficient and accurate non-destructive testing (NDT) methodologies like infrared thermography (Nokes *et al.* 2001, and Halabe *et al.* 2007), microwave testing (Akuthota *et al.* 2004 and Stefen *et al.* 2004) and ultrasonic testing (Giurgiutiu *et al.* 2003 and Kim *et al.* 2007) have been proposed and are routinely employed in reinforced concrete (RC) members retrofitted with FRP. However, all of these experimental techniques require that the vicinity of the damage be known a priori and that the portion of the structure being inspected is readily accessible. As structures become larger and more complex, those techniques become unfeasible and more efficient methods have to be developed. More recently, piezoelectric sensors were introduced into SHM of civil engineering structures and infrastructures as an active sensing technique based on measurement of electrical impedance and elastic waves. In the aspect of impedance method a single PZT is acting both as actuator and sensor. Since the frequency of PZT excitation is very high, the dynamic response of the investigated structure reflects only that of a very local area near the PZT sensor which is very useful to isolate the effect of damage from other far-field changes in loading, stiffness and boundary conditions. The attractive features of the (E/M) admittance technique include its capability of capturing a wide range of structural damage from small to large scale, availability of continuous on-line monitoring, ease of practical application and cost effectiveness. It is interesting to note that, to the present authors knowledge, only very few implementations of the (E/M) admittance technique have been performed on a number of concrete structures retrofitted by FRP laminates (Park *et al.* 2011, and Kim *et al.* 2008). However, in these investigations damage is detected by changes in admittance signatures of smart piezoelectric transducers bonded on the structure. The damage identification has so far been restricted to using non-parametric statistical indices to measure changes in the admittance signatures. These measures, although effective in detecting the existence of damage, fail to correlate the changes in the admittance signatures to information about the location and severity in order to identify the damage. In a recent work of Proidakis (Proidakis *et al.* 2013), a promising advancement of the electro-mechanical admittance-based damage detection technique was proposed by integrating its performance with a guided-wave adaptation.

Computer technology has motivated what used to be a series of complicated mathematical calculations into fairly quick, yet sophisticated, analyses. From this kind of analyses, an expert can optimize process setting design limits in the response. The right design must be chosen in order to fulfill the main objective of the specific problem under investigation. This design is then used to

effectively choose an appropriate number of factors that actually control the dynamic system and contribute to its response. Typically, full-factorial or slightly fractional factorial designs are used to identify both main and interaction effects. Finally, when some of the factors have a curvilinear relationship with some of the responses, an optimization stage is then implemented. Already, popular in the chemical and industrial engineering communities, response surface metamodeling technique is a statistical method used to ‘intelligently’ determine which simulation or physical experiments should be run when resources are scarce (Myers and Montgomery 1995). The method of response surface metamodeling relies on analysis of variance, or ANOVA, to select a few design points out of the full factorial set that efficiently provide the required information about the full response space. Parametric metamodels may then be fit to these selected design data points using regression methods resulting in a polynomial model that relates input to output parameters.

Although response surface metamodeling technique is increasingly employed in various fields related to materials science, its application for structural damage detection and identification is not very usual. A review of the limited literature related to the damage detection and identification using the response surface metamodeling technique can be found in the work of Ratherford *et al.* 2006. They also showed that metamodels were robust to experimental variability and thus, may be used as reduced order models for both linear and nonlinear structural dynamics systems. In the works of County, 2002 for the performance of damage identification using response surface metamodels, stiffness and location (as input damage parameters) and natural frequencies (as output features) were chosen and treated as continuous variables due to optimization difficulties encountered using discrete variables. Finally, after the response surface metamodels have been constructed for each output feature, they were then used in an inverse sense to do damage identification. Cho (2007) employed a damage inspection methodology to predict the accumulated damage in concrete structures and he demonstrated that RSM could be applied to efficiently predict the probability of cyclic freeze-thaw damage.

In the present paper, as a further step, the concept of electro-mechanical admittance-based damage detection technique is integrated with a RSM-based approach to characterize damage rather merely detecting its presence. The focus of this paper is to demonstrate the feasibility of using a response surface metamodeling technique for identifying damage severity in engineering structures with high cost efficiency in modeling and updating. This technique uses statistically analyzed metamodels developed in MATLAB (MATLAB 2012) environment while the required inversion problem was solved by also using global optimization routines of polynomials performed in MATLAB environment. The (E/M) admittance (impedance) signatures were numerically resulted from a finite element analysis using COMSOL 4.2a (COMSOL 2011) commercial software.

2. Electromechanical admittance (EMA) approach

The EMA technique uses piezoelectric materials, such as Lead Zirconate Titanate (PZT), which exhibits the characteristic feature to generate surface charge in response to an applied mechanical stress and conversely, undergo mechanical deformation in response to an applied electric field.

Consider a structural component with a PZT patch bonded on it. The related physical model is shown in Fig. 1 for a square PZT patch of length $2\ell_{\text{PZT}}$ and thickness h_{PZT} .

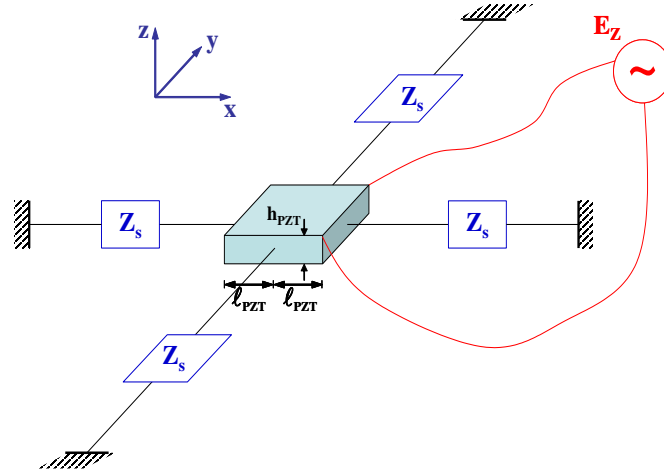


Fig. 1 Model of interaction between PZT and structure

When a harmonic voltage $V=V_0e^{j\omega t}$ with $j=\sqrt{-1}$ is applied in the z -direction, producing an electric field $E=E_0e^{j\omega t}$, an in-plane vibration is induced in both x and y directions. Liang *et al.* (1994) first modeled the 1D PZT-structure electro mechanical interaction, while Bhalla and Soh (2004) extended this approach to 2D structures by using the concept of effective impedance. The constitutive equations of the PZT patch are (Bhalla and Soh 2004)

$$S_x = \frac{1}{\bar{E}_{PZT}}(T_x - \nu_{PZT}T_y) + d_{31}E \quad (1)$$

$$S_y = \frac{1}{\bar{E}_{PZT}}(T_y - \nu_{PZT}T_x) + d_{32}E \quad (2)$$

$$D = \bar{\epsilon}_{33}E + d_{31}T_x + d_{32}T_y \quad (3)$$

where S_x and S_y are strains, T_x and T_y are stresses, $\bar{E}_{PZT} = E_{PZT}(1+n \cdot j)$ is the elastic modulus at zero electric field with E_{PZT} being the elastic modulus of the PZT patch, n is the mechanical loss factor, ν_{PZT} is the Poisson's ratio, d_{31} and d_{32} are the piezoelectric constants in the x and y directions, respectively, $\bar{\epsilon}_{33}^T = \epsilon_{33}^T(1-\delta \cdot j)$ is the dielectric constant at zero stress with ϵ_{33} being the dielectric constant of the PZT patch, D is the electric displacement and δ the dielectric loss factor. If the PZT material is isotropic on the x - y plane, which results in $d_{31}=d_{32}$, the electric displacement in Eq. (3) can be rewritten as

$$D = \bar{\epsilon}_{33}^T E + \frac{d_{31}\bar{E}_{PZT}}{1-\nu_{PZT}}(u' + v' - 2d_{31}E) \quad (4)$$

where $(\)' = \mathcal{G}(\)/\mathcal{G}_x$ and u, v are the displacements responses in x and y direction ,

respectively which can be derived as the solution of the in-plane vibration problem of the PZT patch Liang *et al.* (1994), Bhalla and Soh (2003)

$$\rho_{PZT} \ddot{u} = \frac{\bar{E}_{PZT}}{1 - \nu_{PZT}^2} u'' \quad (5)$$

$$\rho_{PZT} \ddot{v} = \frac{\bar{E}_{PZT}}{1 - \nu_{PZT}^2} v'' \quad (6)$$

where $(\ddot{x}) = \mathcal{G}^2(x) / \mathcal{G}t^2$ and ρ_{PZT} is the density of the PZT patch. The electric current passing through the PZT patch, can be considered to be given by

$$I = j\omega \int_{-\frac{\ell_{PZT}}{2}}^{\frac{\ell_{PZT}}{2}} \int_{-\frac{\ell_{PZT}}{2}}^{\frac{\ell_{PZT}}{2}} D \, dx \, dy \quad (7)$$

Considering that the electric field is defined by

$$E = \frac{V}{h_{PZT}} \quad (8)$$

and that the input voltage V is an AC voltage of 1 Volt (rms) in magnitude, the electric admittance of the PZT patch can be expressed as

$$Y = \frac{I}{V} = j\omega \Sigma Q_i \quad (9)$$

where ΣQ_i is the total charge over the whole surface of the PZT patch.

Then, to fully capture the coupled piezoelectricity-elasticity interfacial problem between PZT patch and host structure a displacement continuity procedure should be conducted by matching the displacements at the PZT's boundary surface with the same position of the host structure.

3. Response surface methodology (RSM)

The structural engineering problems are governed by factors such as material properties, loads and member dimensions. In view of structural damage condition assessment, there is need to quantify and compare the importance of each one of those factors. The conventional methodology of changing one factor at a time and investigating the effect of this factor on the response is a quite complicated technique, particularly in a multivariable system or if more than one response is of importance. Response surface methodology (RSM) is used when only a few significant factors are involved in the optimization without the need for studying all possible combinations experimentally. Further, the input levels of the different variables for a particular level of response may also be determined.

RSM comprises a set of statistical methodologies for model building and model exploitation. By careful design and analysis of experiments (simulations), it seeks to relate a response or output

variable to the levels of a number of predictors of input variables that affect it. It allows calculations to be made of the response at intermediate levels which were not experimentally investigated and show the direction in which to move if we wish to change the input levels so as to decrease or increase the response.

The design procedure of RSM is as follows (Charles and Kenneth 1999), (Box, Hunter and Hunter 1978):

- Designing of a series of experiments (simulation) for adequate and reliable measurement of the response of interest.
- Developing a polynomial metamodel of the second order response surface with the best fittings.
- Finding the optimal set of experimental parameters that produce a maximum or minimum value of response.
- Representing the direct and interactive effects of process parameters through two or three dimensional plots.
-

RSM is based on the assumption that it is possible to define the dependency between variables X_i of the action called factors (input) and the response of the response (output) Y through an approximation function of the form:

$$Y = f(X_1, X_2, X_3, \dots, X_k) \quad (10)$$

The objective is to optimize the response variable Y . It is assumed that the independent variables are continuous and controllable by simulations with negligible errors. Usually a second-order metamodel is utilized in response surface methodology

$$Y = b_0 + \sum_{i=1}^k b_i X_i + \sum_{i=1}^k b_{ii} X_i^2 + \sum_{i=1}^{k-1} \sum_{j=2}^k b_{ij} X_i X_j + \varepsilon \quad (11)$$

where $X_1, X_2, X_3, \dots, X_k$ are the input factors which influence the response Y ; $b_0, b_{ii}(i=1,2,\dots,k), b_{ij}(i=1,2, \dots,k ; j=1,2,\dots,k)$ are unknown parameters and ε is a random error.

The b coefficients, which could be determined in the second-order metamodel, are obtained by the least square method. In general Eq. (10) can be written in matrix form

$$Y = bX + \varepsilon \quad (12)$$

$$b = (X'X)^{-1} X'Y \quad (13)$$

where X' is the transpose of the matrix X and $(XX')^{-1}$ is the inverse of the matrix $X'X$. The number of input parameters of the second-order polynomial may be unlimited. If more input parameter levels are included in a model, then a higher order metamodel may be constructed. The more levels incorporated into a design, the larger the design will be for the same resolution of a design with fewer input parameter levels.

4. Limit states for reinforced concrete (RC) retrofitted with CRFP

The successful extension of the RC component's service life through externally bonded FRP flexural or shear strengthening elements requires a condition of perfect bonding between the FRP and the structure. However failure of FRP strengthened RC members may take place through one or more mechanisms depending of the member and strengthening parameters. Fig. 2 shows the typical failure modes of beams or plates having bonded FRP reinforcement on the soffit. These failure modes are usually closely related to the concrete crack development and are dominated by either midspan debonding initiated by flexural and/or shear cracks (Fig. 3) or end peeling initiated high bond shear stresses at the end of bonded reinforcement (Fig. 4).

Since the FRP debonding procedure prevents the full ultimate strength capacity of RC structural members from being utilized, it is of great importance to identify the initiation and development of FRP debonding.

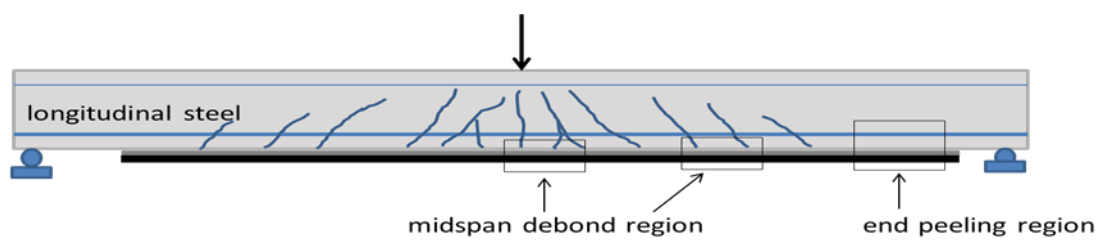


Fig. 2 Typical failure modes in RC structural components retrofitted with externally bonded FRP

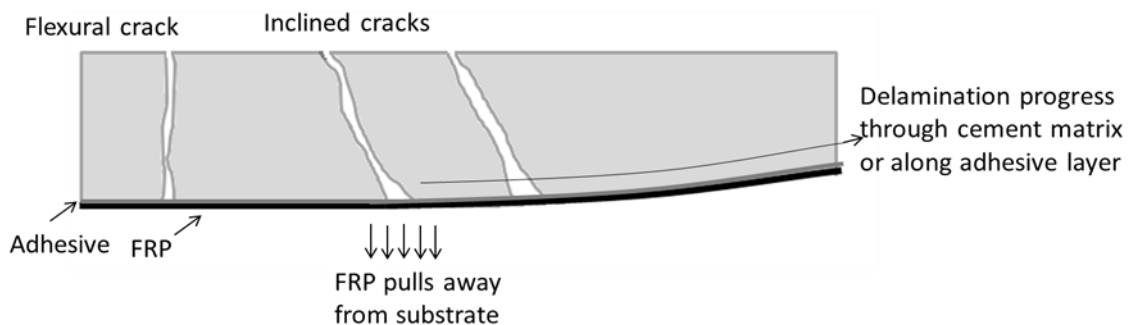


Fig. 3 RC beam debond failure states at midspan

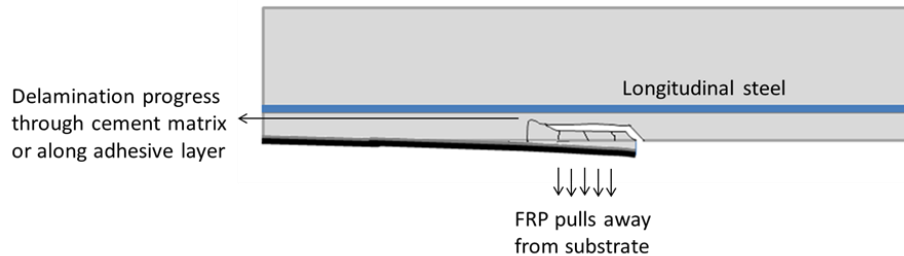


Fig. 4 FRP end peeling at the RC beam shear span

5. FRP debonding identification through finite element simulation

5.1 Methodology

Since in real engineering applications it would be impractical or even, in some times, impossible to actually produce a great number of damaged structures in order to be used for training metamodels, computer simulations rather than experimental in situ investigations will be used here to build response surface models to perform the present damage identification. The test specimen consists of a RC beam with an externally bonded FRP strip as shown in Fig. 5. The RC beam is 0.2 m deep and 0.3 m wide. Its length is 4 m but due to symmetry only half of its length is modeled. It is reinforced with four upper and four lower longitudinal reinforcing steel bars at a spacing of 75 mm as primary flexural reinforcement. No additional shear reinforcement in the form of stirrups was included in the investigated RC beam model. The soffit-applied high modulus carbon FRP (CFRP) preformed strip is 0.20 m wide, 1.4 mm thick and is applied over the middle 3 m of the RC beam specimen using a relative low modulus epoxy-based structural adhesive (FX776 glue).

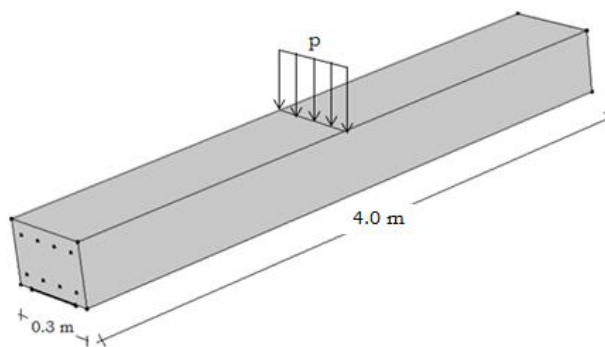


Fig. 5 FRP reinforced RC beam overall structural system

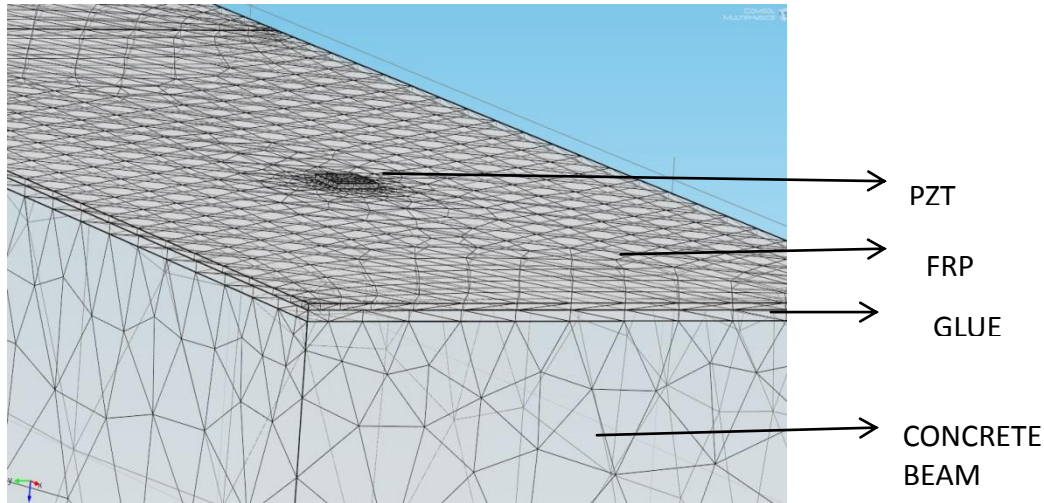


Fig. 6 Details for the FE simulation setup model for FRP-reinforced RC beam

In addition, the overall RC beam system model includes four Lead Zirconate Titanate (PZT5H) square patches (10 mm x 10 mm x 0.2 mm thick) that were attached on the centerline of the free surface of the FRP as shown in the drawing detail of Fig. 6. The location of the first PZT is 100 mm (PZT1) from the middle of the RC beam while the spacing between PZTs is 200 mm. The second PZT is termed as PZT2. In the present study, every PZT acts as an "active" local electromechanical admittance sensor. The RC beam model is loaded at its midspan under a uniformly distributed across its entire width load P . The frequency range of 10 kHz to 400 kHz is commonly used for the electromechanical admittance method. In the present study, a frequency range between 75 kHz and 150 kHz was chosen because it contains a good dynamic interaction between PZT and RC beam structure with multiple resonant peaks. The PZT electromechanical admittance spectrum monitoring process was as follows:

- First, admittance computations were taken by using frequency domain finite element analysis at the predefined frequency band for the soundness state of the RC beam model without any load P ($P=0$).
- Then, a stationary finite element procedure is applied taking into account that the RC beam model is loaded by gravitational loading plus a static-like distributed load of magnitude $P=1.6$ kN/m.
- The computed finite element strains at model nodes are then used as initial conditions to a subsequent frequency domain analysis to obtain the electromechanical admittance spectrum at load $P=1.6$ kN/m.
- The sequence above was repeated until the load reach a value of $P=48$ kN/m.

As described above, the failure modes for FRP debonding are usually closely related to the concrete damage development. Taking this into account, we assumed that it is reliable to consider that in order to monitor the FRP debonding in the inspected RC beam model, all we just need is to monitor the damage development occurring in the concrete core continuum of the overall

structural RC beam model during the above mentioned loading procedure. Thus here, it is assumed that all materials except concrete will almost behave in a linear elastic mode up to the failure. However, concrete, under multi-axial combinations of loading behaves in a different way from that observed in uniaxial conditions. Especially, the behavior of concrete in cases of massive structural applications, or reinforced concrete structural components confined by either steel, FRP or combination of both must be carefully analyzed. For the purposes of the present study, we assumed that the load-carrying capacity of concrete material is predicted by utilizing a four-parameter Ottosen-type failure surface (Montoya *et al.* 2006) which can be represented by the following set of equations

$$a \frac{J_2}{f_c'^2} + \lambda \frac{\sqrt{J_2}}{f_c'} + b \frac{I_1}{f_c'} - 1 = 0; \quad (f_c' > 0) \quad (14)$$

$$\lambda = k_1 + k_2 \cdot \cos 3\theta \quad (15)$$

where the parameters a , b , k_1 and k_2 , and the stress invariants I_1 , J_2 and J_3 can be obtained in terms of the principal concrete strengths

$$\cos 3\theta = \frac{3\sqrt{3}}{2} \frac{J_3}{J_2^{3/2}}; \quad J_2 = \frac{1}{2}(s_1^2 + s_2^2 + s_3^2) \quad (16)$$

$$J_3 = \frac{1}{2}(s_1^3 + s_2^3 + s_3^3); \quad I_1 = (f_{c1} + f_{c2} + f_{c3}) \quad (17)$$

$$s_i = f_{ci} - \frac{1}{3}I_1; \quad i=1,2,3 \quad (18)$$

For the present study, to reproduce the Ottosen-type failure modes of concrete, we assumed that the uniaxial concrete compressive strength f_c' is 20 MPa, the a parameter is 1.3, the b parameter is 3.2, while the parameters k_1 and k_2 are equal to 11.8 and 0.98, respectively.

For the finite element analysis of the inspected RC beam retrofitted by FRP we utilized the COMSOL Structural Mechanics finite element module (COMSOL 2011). A constant regular discrete mesh is implemented for the numerical modeling. Furthermore, the constitutive relations of materials are formulated at the element integration points. To increase the efficiency of numerical results, the aspect ratio of elements are kept equal to one for solid concrete and adhesive materials. For the overall RC beam structural model, including the concrete core, retrofitting FRP laminates and bonding adhesive interface, almost 7000 solid brick finite elements were used that can consider geometrical effects, plasticity and damaged deformations. For numerical simplification of the investigated model, only half of the beam model is modeled as a result of symmetric boundary conditions. The modeled RC beam is assumed to be simply supported at its end. The steel reinforcements are treated as two node truss elements network embedded discretely in concrete brick finite elements and the full bond effect between concrete and steel elements are imposed by integration and nodal constraints. The typical finite element idealization of the investigated RC beam model is presented in Fig. 7 as seen from the bottom.

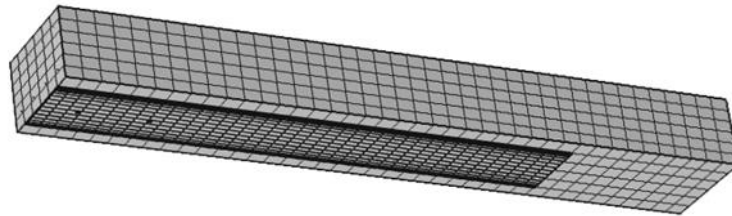


Fig. 7 Typical finite element mesh for the half length of RC concrete beam (bottom view)

A common measure of inelastic deformation is the volumetric plastic strain which is growing as the material is actively yielding. Thus, in our analysis, whenever the state of stress in concrete core material is reaching the Ottosen-type failure surface, it can be considered that a state of damage is occurred. Finally, taking into account that the volume integral of volumetric plastic strain across a predefined 3-D geometrical zone gives a reliable measure of the volume of damaged concrete material inside this zone, we assumed that if this volume integral of the volumetric plastic strain results to a value greater than zero it constitutes a "damaged" state to the overall RC beam structural system. As described above, two geometric zones are of great importance in FRP retrofitted RC structural components under flexural loading: near the midspan of the specimen where damage may initiate by flexural and/or shear cracks and near the end of FRP bonded reinforcement due to end peeling initiated by high shear stresses. Thus, for the present damage identification purposes we introduce two geometric zones as shown in Fig. 8(a)) Geometric Zone I defined as the volume being between the midspan and the points located in a distance smaller than 0.5 m away from the midspan, and b) Geometric zone II between the points located in a distance of 1.25 m away from the midspan and those points located in a distance of 1.75 m away from the midspan.

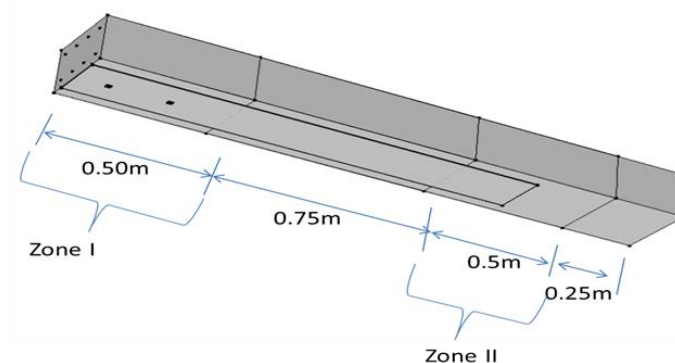


Fig. 8 Plastic zones I and II of the RC structural member

Various kinds of damage indices have been developed for health monitoring of civil structures in recent years. For the quantitative assessment of the concrete failure, a damage metric based on the average difference square metric (Raju 1997) which is given by the following mathematical formulation

$$ASD = \sum_{i=1}^n \text{Re}[(Y_{1,i}) - (\text{Re}(Y_{2,i}) - \delta)]^2 \quad (19)$$

where $\delta = \text{Re}(\bar{Y}_1) - \text{Re}(\bar{Y}_2)$, ASD is the average difference square metric, $\text{Re}(Y_{1,i})$ is the real part of the electromechanical admittance spectrum of a PZT patch computed under healthy state conditions at the frequency interval i , $\text{Re}(Y_{2,i})$ is the real part of a subsequent electromechanical admittance spectrum at a frequency point i , $\text{Re}(\bar{Y}_1)$ is the average value of the initial admittance spectrum curve and $\text{Re}(\bar{Y}_2)$ is the average value of a subsequent admittance spectrum curve.

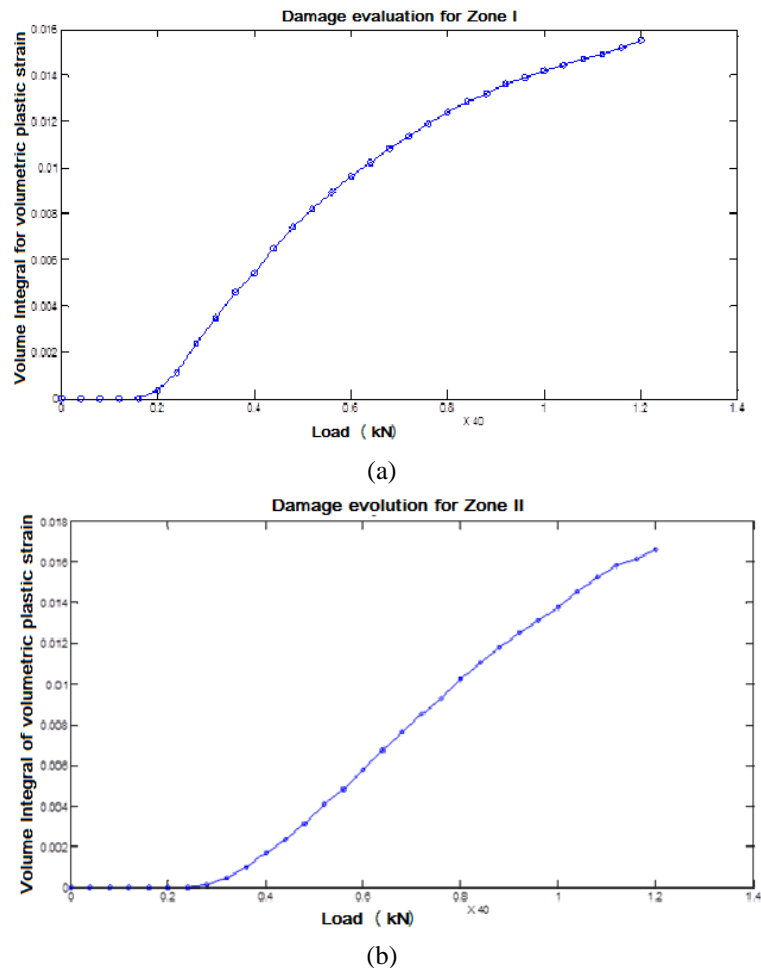
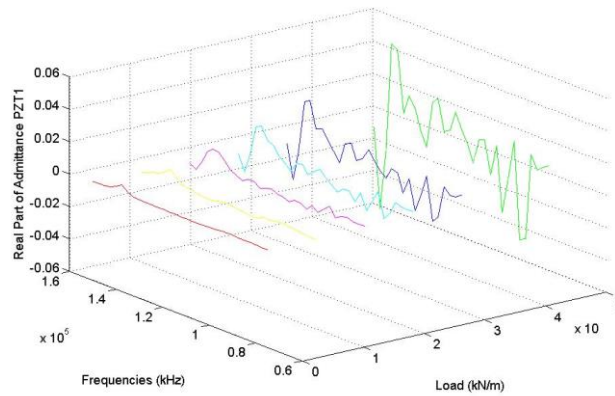
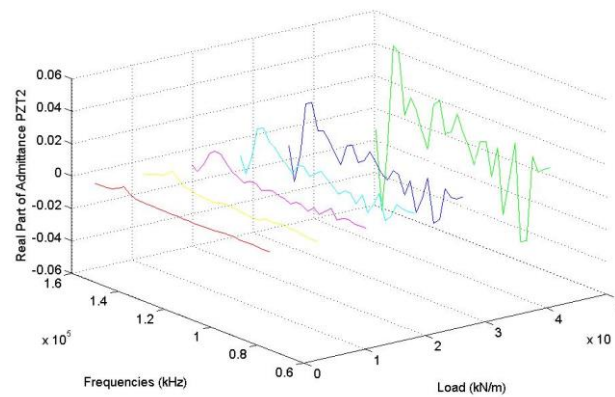


Fig. 9 (a) Damage evolution for Zone I as a function of load and (b) Damage evolution for Zone II as a function of load



(a)



(b)

Fig. 10 (a) Frequency spectrum of the real part of electromechanical admittance at PZT1 as a function of load and (b) Frequency spectrum of the real part of electromechanical admittance at PZT2 as a function of load

To simulate the monitoring process of the inspected FRP strengthened RC beam specimen, the loading procedure described above was followed by gradually increasing the load magnitude. Then, through the COMSOL nonlinear stationary finite element analysis, the damage (plastic) zone strain evolution for both zone I and zone II is obtained and plotted in Figs. 9(a) and 9(b). From the inspection of Figs. 9(a) and 9(b), it can be concluded that an intact damage is computed at a loading magnitude value of $0.16 \times 40 \text{ N/m} = 6.4 \text{ kN/m}$ for zone I and $0.28 \times 40 = 11.2 \text{ kN/m}$ for zone II. This important values, along with Figs. 9(a) and 9(b) will be used as references to verify the proposed damage monitoring methodology. After each stationary finite element analysis, a frequency domain finite element analysis was performed in order to compute the electromechanical admittance spectrum for a frequency sweep between 75 kHz and 150 kHz with a frequency step of 2.5 KHz. Typical electromechanical admittance spectrum curves as obtained for some specific loading steps for both PZT1 and PZT2 are presented in Figs. 10(a) and 10(b).

5.2 Response surface methodology

Table 1 ASD Response and Damage Input values as a function of loading

Load (P) x 40 kN	ASD at PZT1 (Y1 Response)	ASD at PZT2 (Y2 Response)	Damage at zone I (Input X1)	Damage at zone II (Input X2)
0,00	0,000000E+00	0,000000E+00	0	0
0,04	2,312216E-06	1,876932E-06	0	0
0,08	2,312000E-06	1,876926E-06	0	0
0,12	2,311783E-06	1,876920E-06	0	0
0,16	2,311565E-06	1,876914E-06	0	0
0,20	6,032301E-06	1,784687E-06	0,000358	0
0,24	2,528423E-05	6,280326E-06	0,001137	0
0,28	2,660084E-05	1,805221E-05	0,002384	0
0,32	2,517160E-05	1,654753E-05	0,003494	0
0,36	2,353018E-05	2,027420E-05	0,004593	0
0,40	1,975860E-05	1,843320E-05	0,005425	0
0,44	3,328072E-05	9,846528E-06	0,006516	0
0,48	3,927879E-05	1,954584E-05	0,007423	0
0,52	4,586687E-05	2,295391E-05	0,008199	0
0,56	5,132274E-05	2,819522E-05	0,008928	2,21E-05
0,60	4,756826E-05	2,928642E-05	0,009629	2,21E-05
0,64	5,258334E-05	4,174439E-05	0,010204	2,39E-05
0,68	5,014364E-05	3,390304E-05	0,010823	2,57E-05
0,72	6,216181E-05	3,152707E-05	0,011365	3,14E-05
0,76	5,724980E-05	3,332741E-05	0,011913	8,62E-05
0,80	6,923589E-05	3,855020E-05	0,01241	0,000153
0,84	6,946977E-05	3,827516E-05	0,012844	0,000222
0,88	8,695740E-05	3,953251E-05	0,013202	0,000312
0,92	9,604465E-05	4,728842E-05	0,01362	0,000415
0,96	9,207367E-05	4,178853E-05	0,01388	0,000612
1,00	8,985253E-05	4,352975E-05	0,014192	0,000766
1,04	1,013144E-04	4,779052E-05	0,014447	0,000931
1,08	1,066470E-04	5,339120E-05	0,014694	0,001107
1,12	1,049975E-04	5,962124E-05	0,014898	0,00132
1,16	1,043967E-04	7,115063E-05	0,015193	0,001487
1,20	9,618350E-05	7,280730E-05	0,015519	0,001762

Considering the values for the ASD damage metrics calculated for the two PZT patches as response values (termed as ASD1 for PZT1 and ASD2 for PZT2, respectively) for each one of the 30 loading steps, and the volume integrals of the volumetric plastic strains as obtained for zone I and zone II under each one of the 30 loading steps as input values (termed as X1 and X2, respectively), Table 1 is obtained.

Taking into account the results presented in Table 1, one can easily observe that when the time instant of damage in zone I is raised, the calculated admittance values at PZT1 which is located in a closer distance to the damage zone I area than PZT2 is greatly affected as compared to that of PZT2. And the same interesting point is derived but in an inverse manner for the time instant of damage in zone II where PZT2 is in a closer distance than PZT1. These results prove how much effective is EMA technique to damage localization. To perform the proposed response surface methodology and create the response surfaces (RS), quadratic polynomials showing good regression accuracy were employed and expressed in the following expanded form

$$ASD1 = b_0 + b_1X_1 + b_2X_2 + b_3X_1X_2 + b_4X_1^2 + b_5X_2^2 \quad (20)$$

$$ASD2 = b_6 + b_7X_1 + b_8X_2 + b_9X_1X_2 + b_{10}X_1^2 + b_{11}X_2^2 \quad (21)$$

By the use of the Least-square Method as performed in MATLAB software platform (MATLAB 2011), the regression coefficient of Eqs. (20) and (21) was obtained and the RS of second order is shown as

$$ASD1 = 4,8771x10^{-6} + 0,005X_1 + 0,0814X_2 - 1,2514X_1X_2 - D1 = \\ = b_0 + b_1X_1 + b_2X_2 + b_3X_1X_2 + b_4X_1^2 + b_5X_2^2 \quad (22)$$

$$ASD2 = 2.4645x10^{-6} + 0.0031X_1 + 0.1603X_2 \\ -12.0972X_1X_2 - 0.0311X_1^2 - 26.2930X_2^2 \quad (23)$$

Figs. 11 and 12 below present the two 3-D response surface plots generated, at PZT1 and PZT2 locations, respectively, in terms of both two zone I (X1) and zone II (X2) damage levels.

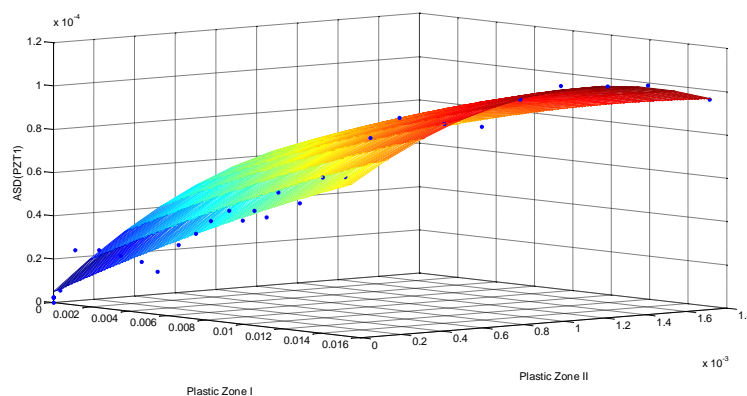


Fig. 11 3-D RSM plots of ASD index at PZT₁

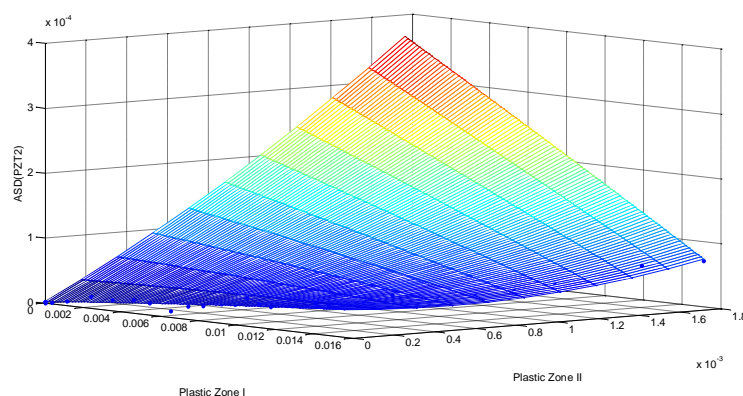


Fig. 12 3-D RSM plots of ASD index at PZT₂

5.3 Damage identification inverse problem

At the final stage of the present damage identification methodology, after the response surface metamodells have been constructed they should be used in an inverse sense to do damage identification. The problem: “Knowing the output values of the average difference square metric by retrieving electromechanical admittance data at specific PZT patch locations, what were the input damage level parameters at specific zones that may lead to such values ?” must be analyzed and solved accordingly.

This problem was first attempted using a simple error minimization scheme performing the MATLAB *fminsearch* routine (MATLAB 2012). This simple optimization scheme stopped once a minimum between the actual and the predicted output feature value of the real part of the electromechanical admittance was achieved. But, it was very easy to prove that these minimum values were not unique since this kind of inverse problems has many local minima. Thus, the advanced MATLAB routine *Snobfit- Stable Noisy Optimization by Branch and Fit* (<http://www.mat.univie.ac.at/~neum/software/snobfit/>) (Huyer and Neumaier 2006) has been used to solve the global optimization problem of the multivariable present work. It may generate a series of lower bounds monotonically converging to the global optimum at low computational cost.

To test how well the global optimization procedure through *Snobfit* routine worked, a set of runs was executed which includes 10 original run points. That is, knowing the 60 output feature values (2 PZT locations x 30 pre-selected loading steps) of ASD damage indices, could the damage input level value at zone I and zone II be identified? The damage identification results are shown in Table 2, with the damage level to be predicted by the *Snobfit* optimization routine. Results are also shown in Figs. 13 and 14, in the form of two plots of actual damage level versus predicted damage level from the global optimization procedure of *Snobfit* routine.

It can be observed that damage predictions are much more successful at zone I₃. This is an

expected result since it is well known that locations closer to the PZT sensor locations are predicted better than locations far away from them. It can be also seen in these figures that the present inverse formulation captures better the main trend for the predicted damage level in the simulated RS points than the points that are not in the RS design set. One possible reason for higher damage identification error might be because continuous input damage variables were used to represent discrete damage parameters.

Table 2 Set of damage identification results

Run	Original Damage Input		Predicted Damage Input by <i>Snobfit</i>	
	X_1	X_2	X_1	X_2
1	0	0	0.0002	0.0001
2	0.0011	0	0.0024	0.0005
3	0.0046	0	0.0053	0.0001
4	0.0089	2.21e-5	0.009	0.0004
5	0.0108	2.57e-5	0.0118	0.002
6	0.0119	8.6e-5	0.0122	0.0017
7	0.0144	2.2e-4	0.0138	0.002
8	0.0142	7.66e-4	0.0139	0.0011
9	0.0149	0.0013	0.0142	0.0018
10	0.0152	0.0015	0.016	0.0018

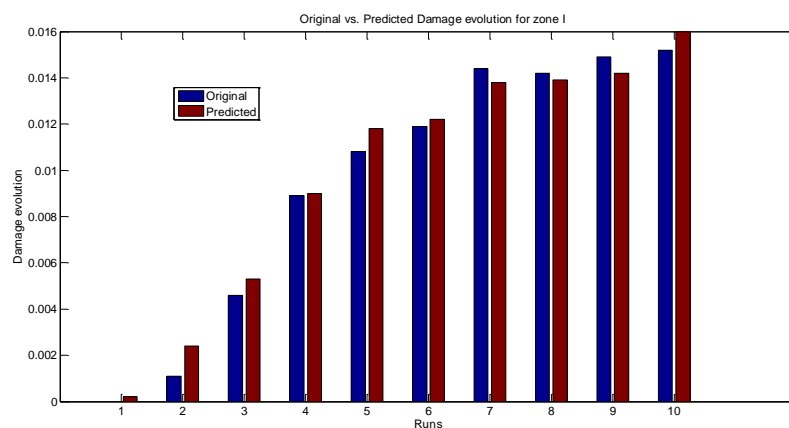


Fig. 13 Comparison between original and predicted values for Damage evolution in Zone I

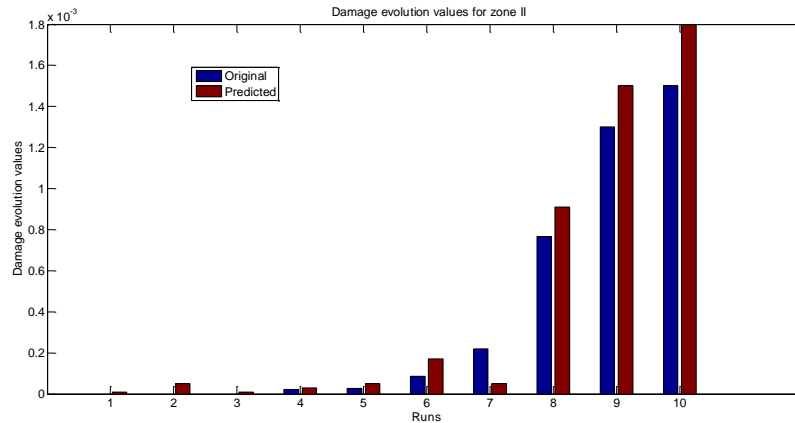


Fig. 14 Comparison between original and predicted values for Damage evolution in Zone II

6. Conclusions

With the combination of finite element method and Response Surface Methodology, analysis of damage parameters effect was greatly simplified and the simulation process of damage identification in FRP retrofitted RC structural components was made efficient. The main advantage of the proposed approach is its computational simplicity to detect and localize damage in CFRP-strengthened concrete structures without requiring numerous diagnostic database sets. Any complicated inelastic damage zone imposed in concrete core or in CFRP outer layer could be easily identified. Having appropriate quadratic response surface metamodels of the input parameter variations is important in analyzing a structure's current state of health and predicting structural behavior in various conditions. The health monitoring process proposed here capitalizes the response surface metamodeling technique for the minimization of the associated prediction error and thus, it can be efficiently used in determining the damage state of a structure. Damage identification was performed by solving an inverse problem using a set of two quadratic response surface polynomials which were trained on 31 RSM simulation runs. Results for all sets of simulations were encouraging with correct trends captured for a number of damage locations.

Acknowledgments

The research described in this paper was financially supported by the European Union (European Social Fund-ESF) and Greek national funds through the Operational Program "Education and Lifelong Learning" of the National Strategic Reference Framework (NSRF) – Research Funding Program : THALES. Investing in knowledge through the European Social Fund.

References

- Akuthota, B., Hughes, D., Zoughi, R., Myers, J. and Nanni, A. (2004), "Near field microwave detection of disbond in fiber reinforced polymer composites used for strengthening concrete structures and disbond repair verification", *J. Mater. Civil Eng. - ASCE*, **16**(6), 540-546.
- Bhalla, S. and Soh, C.K. (2003), "Structural impedance damage diagnosis by piezo-transducers", *J. Earthq. Eng. Struct. D.*, **32**, 1897-1916.
- Bhalla, S. and Soh, C.K. (2004b), "Health monitoring by piezo-impedance transducers I: modeling", *J. Aerospace Eng.*, **17**, 154-165.
- Charles, R.H. and Kenneth, V.T. (1999), *Fundamental concepts in the design of experiments*, University Press, Oxford.
- Cho, T. (2007), "Prediction of cyclic freeze-thaw damage in concrete structures based on response surface method", *Constr. Build. Mater.*, **21**(12), 2031-2040.
- COMSOL (2011), Ltd, Comsol Multiphysics Modelling 4.2a, www.comsol.com, 2011, Users Guide, London.
- Cundy, A.L. (2002), *Use of response surface metamodels in damage identification of dynamic structures*, Master's Thesis, Virginia Polytechnic Institute and State University.
- Giurgiutiu, V., Harries, K.A., Petrou, M.F., Bost, J. and Quattlebaum, J. (2003), "Disbond detection with piezoelectric wafer active sensors in RC structures strengthened with FRP composite overlays", *J. Earthq. Eng. Eng. Vib.*, **2**(2), 213-224.
- Halabe, U.B., Vasudevan, A., Klinkhachorn, P. and Gangarao, H.V.S. (2007), "Detection of subsurface defects in fiber reinforced polymer composite bridge decks using infrared thermography", *J. Nondestruct. Eval.*, **22**(2-3), 155-175.
- Huyer W. and Neumaier A. (2008), "Snobfit-Stable noisy optimization by branch and fit", *ACM T. Math. Software*, **35**(2), doi>10.1145/1377612.1377613.
- Kim, S.B., Kim, J.H., Nam, J.W., Kang, S.H. and Byeon, K.J. (2008), "Bond-slip model of interface between CFRP sheets and concrete beams strengthened with CFRP", *Korea Concrete Inst.*, **20**(4), 477-486.
- Kim, S.D., In, C.W., Cronin, K.E., Sohn, H. and Harries, K.A. (2007), "A reference-free NDT technique for debonding detection in CFRP strengthened RC structures", *J. Struct. Eng. - ASCE*, **8**, 1080-1091.
- Liang, C., Sun, F.P. and Rogers, C.A. (1994), "Coupled electro-mechanical analysis of adaptive material systems determination of the actuator power consumption and system energy transfer", *J. Intel. Mat. Syst. Str.*, **5**(1), 15-20.
- MATLAB, The Mathworks Inc. U.S. (2012), www.mathworks.com., 2012, Users Guide.
- Mohcene Boukhezar, Mohamed Laid Samai, Habib Abelhak Mesbah and Hacene Houari (2013), "Flexural behaviour of Reinforced low-strength Concrete Beams strengthened with CFRP plates", *Struct. Eng. Mech.*, **47**(6), -819-838.
- Myers, R.H. and Montgomery, D.C. (1995), *Response Surface Methodology*, John Wiley and Sons, Inc., New York, NY.
- Nokes, T.R. and Hawkins, G.F. (2001), *Infrared inspection of composite reinforced structures*, Ohio DOT, OH, 2001: <http://www.dot.state.oh.us/research/2001/Structures/14688-FR.pdf>
- Oehlers, D.J. (2006), "Ductility of FRP plated flexural members", *Cement Concrete Compos.*, **28**(10), 898-905.
- Park, S., Kim, J.W., Lee, C.G. and Park, S.K. (2011), "Impedance-based wireless debonding condition monitoring of CFRP laminated concrete structures", *NDT&E Int.*, **44**, (232-238).
- Providakis, C.P., Stefanaki, K.D., Voutetaki, M., Tsompanakis, J. and Stavroulaki, M. (2013), "Damage detection in concrete structures using a simultaneously activated multi-mode PZT active sensing system", *Struct. Infrastruct. E.*, (submitted).
- Raju, V. (1997), *Implementing impedance-based health monitoring*, MSc thesis, Virginia Polytechnic Institute, Blacksburg, Virginia, USA.

- Rutherford, B.M., Swiler, L.P., Paez, T.L. and Urbina, A. (2006), "Resposne surface (meta-model) methods and applications", *Proceedings of the 24th Int. Modal Analysis Conf.*, St. Louis.
- Shih, J.K.C., Tann, D.B., Hu, C.W., Delap, R. and Andreou, E. (2003), "Remote sensing of air blisters in concrete-FRP bond layer using IR thermography", *Int. J. Mater. Prod. Tec.*, **19**(1-2), 174-187.
- Stephen, V., Kharkovsky, S., Nadakuduti, J. and Zoughi, R. (2004), "Microwave field measurement of delaminations in CFRP concrete members in a bridge", *Proceedings of the Worls Conference on Nondestructive Testing (WCNDT)*, Montreal, Canada.

CC